Appendix for 'Rapid endotheliitis and vascular damage characterize SARS-CoV-2 infection in a human lung-chip model'.

Table of contents

Appendix Fig. S1.

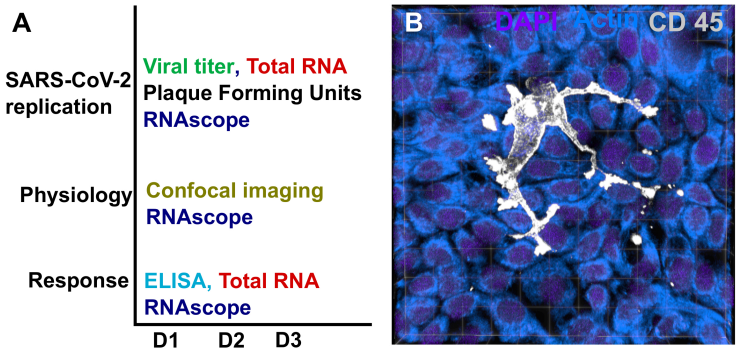

(**A**) An overview of the techniques used to characterize viral replication, physiological changes, and the cellular responses in the LoC over 3 days post infection. (**B**) 3D view of the epithelial layer of an uninfected control LoC reconstituted with CD14+ macrophages added to the epithelial side. Macrophages are identified via an anti-CD45 antibody (grey), actin and nuclear labelling are labelled in azure and electric indigo LUTs respectively.

Appendix Fig. S2.

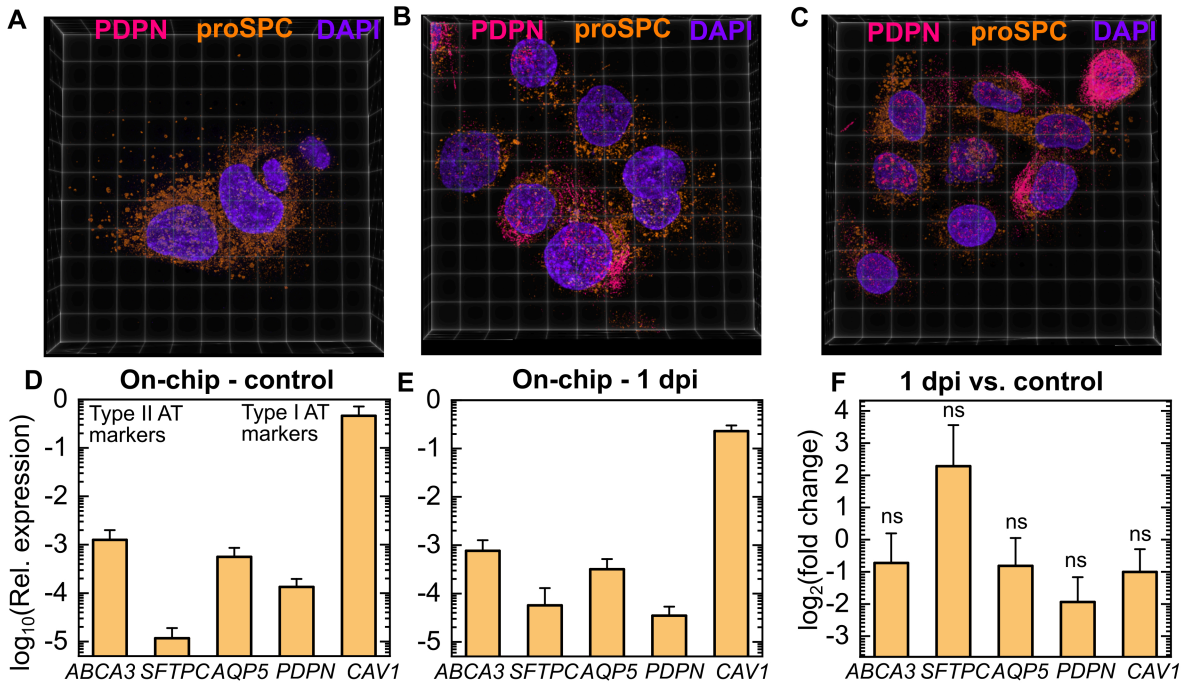

(**A-C**) 3D views of individual alveolar epithelial cells at passage 3. Lamellar bodies characteristic of type II alveolar epithelial cells are identified via an anti-pro-SPC antibody (shown in amber), type I alveolar epithelial cells were identified via an anti Podoplanin antibody (*PDPN*, shown in pink). Nuclear labelling is shown in electric indigo. (**D, E**) Plots of the expression of type II AT markers (*ABCA3*, *SFTPC*) and type I AT markers (*AQP5*, *PDPN*, *CAV1*) relative to *GAPDH* expression from cells in the epithelial layer of (**D**) uninfected controls (n=3 biological replicates) and (**E**) infected LoCs at 1 dpi (n=3 biological replicates for *ABCA3*, *PDPN*, and *CAV1*, and n=4 biological replicates for *SFTPC* and *AQP5*). (**F**) Plots of the fold change in AT markers from the epithelial layers of the LoCs in (**D**) and (**E**). In all plots, the bar represents the mean, and the error bars the standard deviation. P-values are calculated using a one-way Kruskal-Wallis ANOVA test.

Appendix Fig. S3.

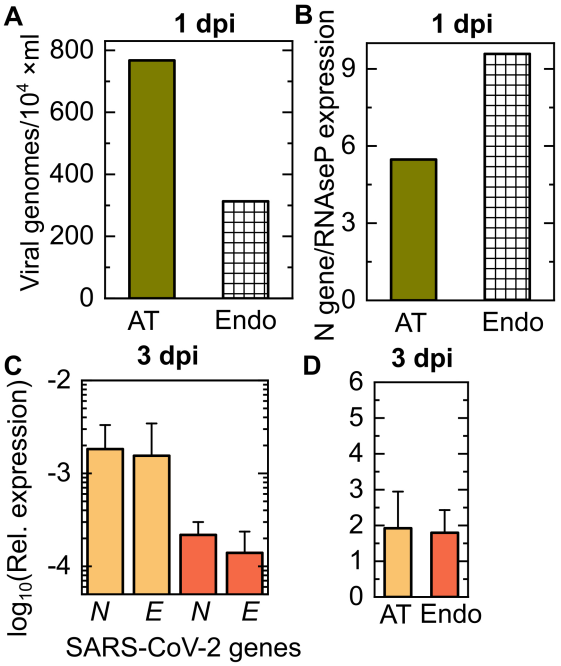

(**A**) Quantification of the numbers of viral genomes detected in the total RNA obtained from the apical and vascular channels respectively of an infected LoC without macrophages at 1 dpi. (**B**) Intracellular viral RNA levels at this timepoint relative to levels of the eukaryotic housekeeping gene *RNaseP. (***C**) Quantification of the intracellular levels of transcripts for the *SARS-CoV-2 N* and *SARS-CoV-2 E* genes in the epithelial and endothelial layers of infected LoCs at 3 dpi (n=3 biological replicates) relative to expression of the eukaryotic housekeeping gene GAPDH. (**D**) SARS-CoV-2 *N:* SARS-CoV-2 *E* ratio in the epithelial and endothelial layers of the infected LoCs shown in (**C**). The bars represent the mean value, and the error bars represent the standard deviation.

Appendix Fig. S4.

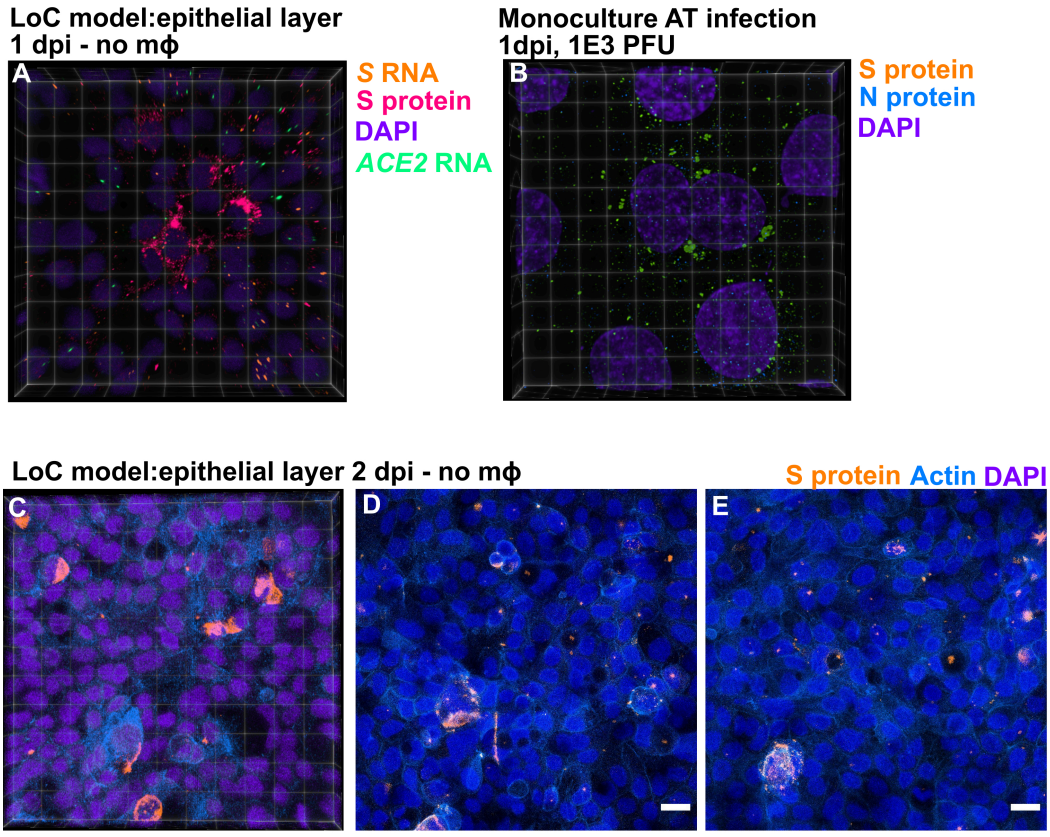

(**A**) 3D view of a 232 x 232 μm^2 field of view of the epithelial layer of an infected LoC at 1 dpi. Three cells with productive amplification of virions can be identified by the formation of clusters of spike protein (identified via antibody labelling and shown in bright pink LUT) localized in the cytoplasm surrounding the nucleus. *S* RNA and *ACE2* mRNA identified via an RNAscope assay and nuclear labelling are shown in amber, spring green, and electric indigo LUTs respectively. (**B**) 3D view of a 61.4 x 61.4 μm^2 field of view of an alveolar epithelial cell monolayer at 1 dpi. Cells with productive amplification of virions can be identified by the formation of clusters of spike protein (identified via antibody labelling and shown in amber LUT) localized in the cytoplasm surrounding the nucleus. SARS-CoV-2 nucleocapsid (N) protein and nuclear labelling are shown in amber and electric indigo LUTs respectively. 3D view (C) and maximum intensity projections (D, E) of three independent 232 x 232 μm^2 field of view of the epithelial layer of an infected LoC at 2 dpi. Spike protein (identified via antibody labelling), actin staining, and nuclear labelling are shown in amber, azure, and electric indigo LUTs respectively. Scale bars = 20 μm.

Appendix Fig. S5.

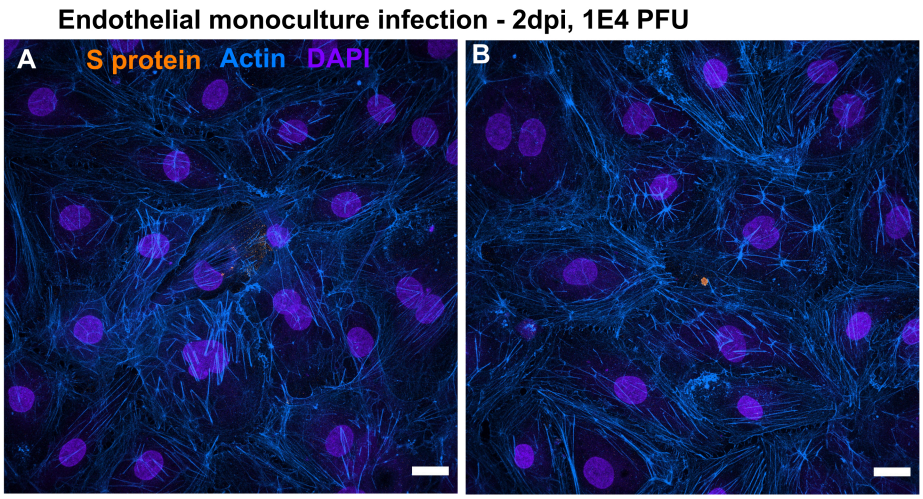

(**A**, **B**) Representative images of endothelial cell infection in a 24 well plate, 2 days post infection with an infectious dose of 1E4 plaque forming units (PFU). An intact monolayer and few signs of SARS-CoV-2 infection are seen. S protein is detected via immunofluorescence, actin staining, and nuclear labelling are shown in amber, azure and electric indigo LUTs respectively. Scale bar = 20 μm.

Appendix Fig. S6.

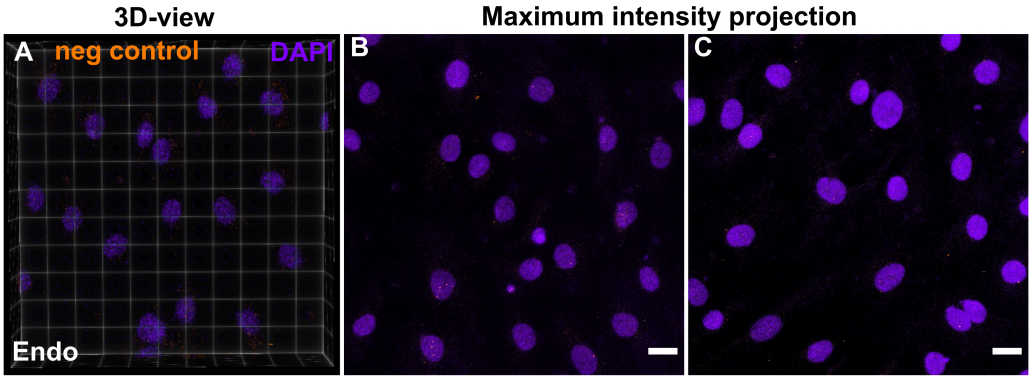

(A) 3D view of a 232 x 232 μm^2 field of view of the endothelial layer of an uninfected LoC at a timepoint corresponding to 3 dpi and processed under the RNAscope protocol with the DapB negative control probe (shown in Amber). (**B**, **C**) Maximum intensity projections of a Z-stack from two independent fields of view 232 x 232 μm^2 field of view from the endothelial layer. The nuclear labelling is false-coloured indigo. Scale bar = 20 μm.

Appendix Fig. S7

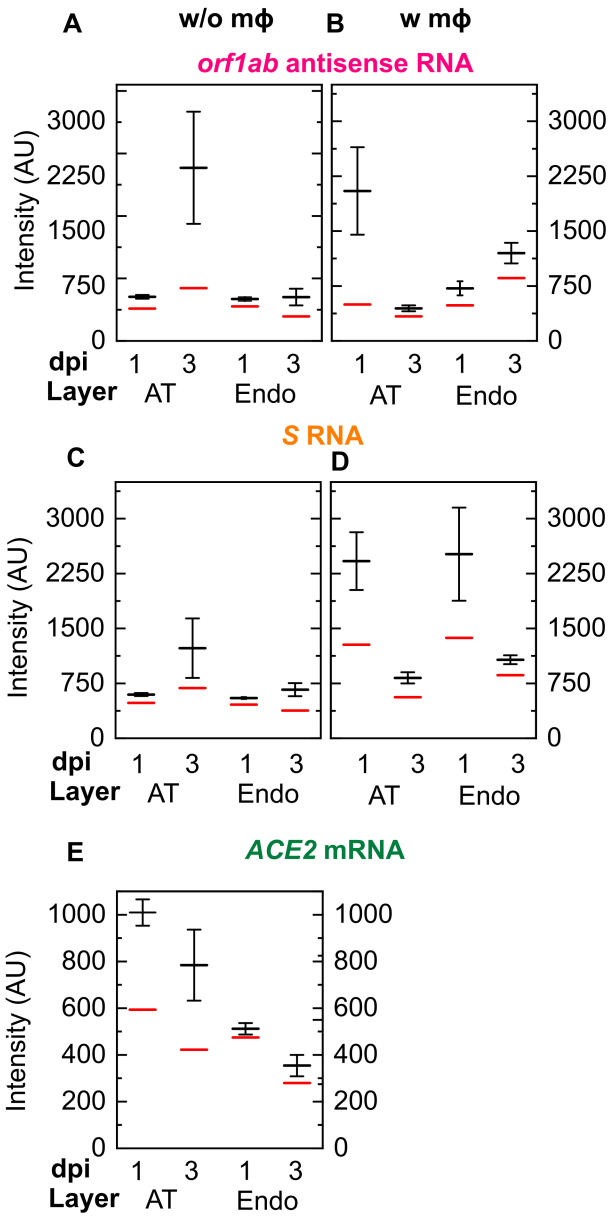

Quantification of viral antisense RNA (**A, B**), viral genomic RNA (**C, D**) and *ACE2* mRNA from pairs of otherwise identical LoCs reconstituted without (**A, C, E**) and with macrophages (**B, D**) and analyzed at 1 and 3 dpi. Plots show the mean (solid black line) and median (solid red line) of the intensity of each spot detected using RNAscope and confocal imaging using identical imaging conditions for all chips. The error bars represent the standard deviation.

Appendix Fig. S8

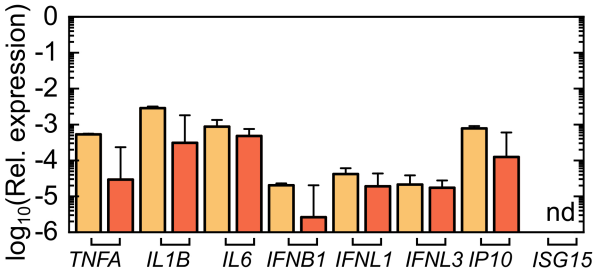

Plot of the expression of the NF-KB related pro-inflammatory cytokines (*TNFA*, *IL1B*, *IL6*), interferon genes (*IFNB1*. *IFNL1*, and *IFNL3*) and interferon stimulated genes (*IP10*, *ISG15*) in cells from the epithelial and endothelial layers of uninfected controls relative to *GAPDH* (n=3 biological replicates). 'nd' refers to not detected. The bars represent the mean, error bars represent the standard deviation.

Appendix Fig. S9

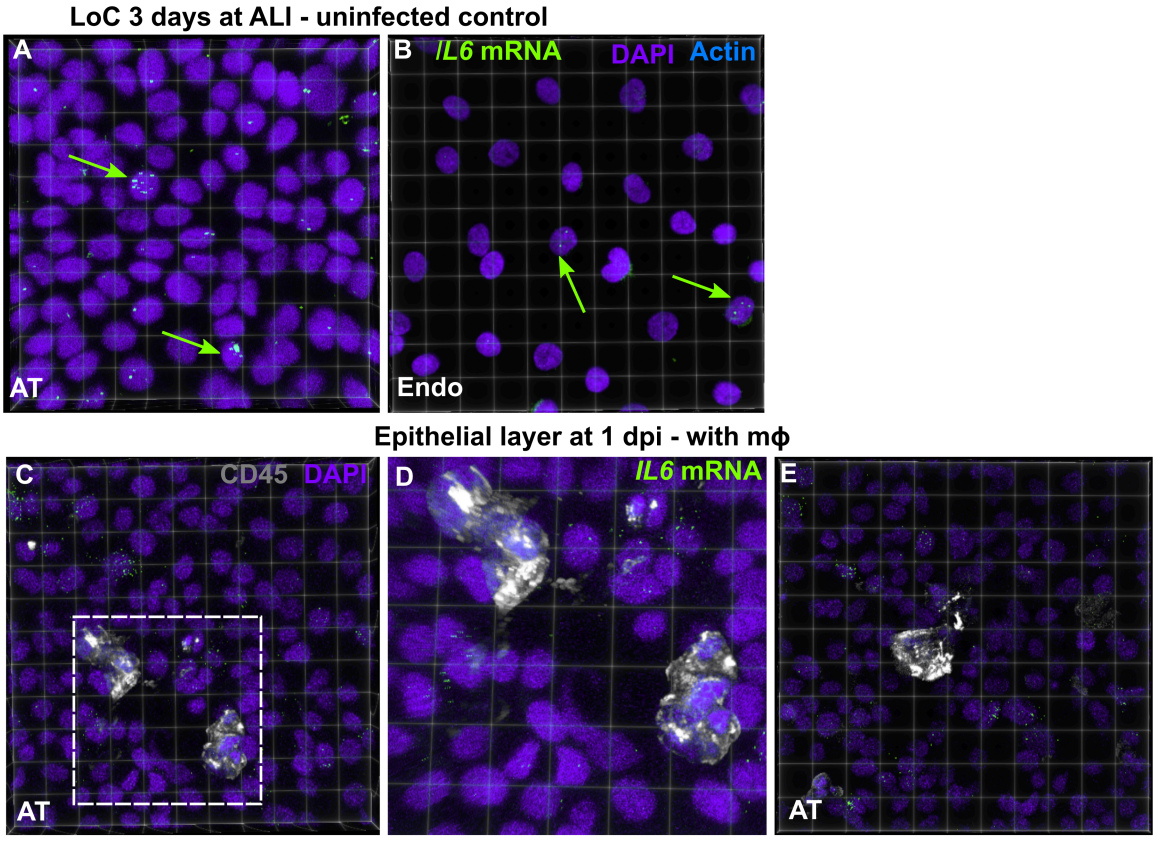

(**A**, **B**) 3D views of representative 155 x 155 µm^2 fields of view of the epithelial layer and endothelial layer corresponding to the images Fig. 1B and 1C. *IL6* mRNA is identified by RNAscope assay and false colored chartreuse (yellow arrows), and nuclear labelling is false colored indigo. Yellow arrows indicate *IL6* mRNA co-localized with the nucleus. (**C, E**) 3D views of two 232 x 232 µm^2 fields of view of the epithelial layer of an infected LoC reconstituted with macrophages at 1 dpi. (**D**) Zoom corresponding to the area marked by the white box in (**C**), macrophages are labelled via an anti-CD45 antibody (gray).

Appendix Fig. S10.

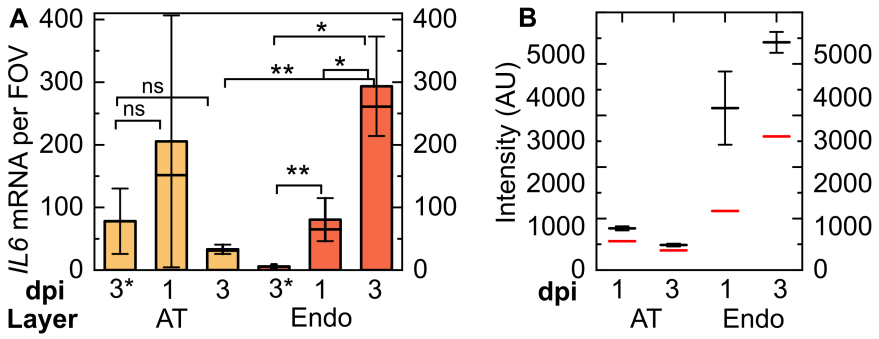

(**A**) Quantification of *IL6* expression in epithelial and endothelial cells from a pair of otherwise identical LoCs analyzed at 1 and 3 dpi, respectively. Plots show the total number of spots in 4-6 fields of view (technical replicates) detected using RNAscope assay using identical imaging conditions for all chips. Bars represent the mean value, the solid line represents the median, and error bars represent the standard deviation. Data from control uninfected LoCs corresponding to the 3 dpi timepoint is labelled '3C'. (**B**) Plots show the mean (solid black line) and median (solid red line) of the intensity of each spot detected using RNAscope and confocal imaging using identical imaging conditions for all chips. The error bars represent the standard deviation. P-values are calculated using the one-way Kruskal-Wallis ANOVA test, * represents p<=0.05, ** represents p<=0.01, ** represents p<=0.001.

Appendix Table S1. Primers used for qRT-PCR characterization of gene expression in this study.

Sequence (5' - 3')	Primer
TAC GGT GTG GCA CCG CTC AAT G	*AQP5* forward
AGT CAG TGG AGG CGA AGA TGC A	*AQP5* reverse
CCA AGG AGA TCG ACC TGG TCA A	*CAV1* forward
GCC GTC AAA ACT GTG TGT CCC T	*CAV1* reverse
GTG CCG AAG ATG ATG TGG TGA C	*PDPN* forward
GGA CTG TGC TTT CTG AAG TTG GC	*PDPN* reverse
GTC CTC ATC GTC GTG GTG ATT G	*SFTPC* forward
AGA AGG TGG CAG TGG TAA CCA G	*SFTPC* reverse
CTT GAC AGT CGC AGA GCA CCT T	*ABCA3* forward
CTC CGT GAG TTC CAC TTG TCC T	*ABCA3* reverse
GTC TCC TCT GAC TTC AAC AGC G	*GAPDH* forward
ACC ACC CTG TTG CTG TAG CCA A	*GAPDH* reverse
TCC ATT GGT CTT CTG TCA CCC G	*ACE2* forward
AGA CCA TCC ACC TCC ACT TCT C	*ACE2* reverse
CCT CTA ACT GGT GTG ATG GCG T	*TMPRSS2* forward
TGC CAG GAC TTC CTC TGA GAT G	*TMPRSS2* reverse
AAC AAC GGC TCG GAC TGG AAG A	*NRP1* forward
GGT AGA TCC TGA TGA ATC GCG TG	*NRP1* reverse
CAT TAC CTG AAG GCC AAG GA	*IFNB1* forward
CAG CAT CTG CTG GTT GAA GA	*IFNB1* reverse
AAC TGG GAA GGG CTG CCA CAT T	*INFL1* forward
GGA AGA CAG GAG AGC TGC AAC T	*IFNL1* reverse
TCG CTT CTG CTG AAG GAC TGC A	*IFNL3* forward
CCT CCA GAA CCT TCA GCG TCA G	*IFNL3* reverse
TGA GGT ACA GGC CCT CTG AT	*TNFA* forward
CCC GAG TGA CAA GCC TGT AG	*TNFA* reverse
CCA CCT CCA GGG ACA GGA TA	*IL1B* forward
AAC ACG CAG GAC AGG TAC AG	*IL1B* reverse
ATT TGC CGA AGA GCCC TCA G	*IL6* forward
CCC CTG ACC CAA CCA CAA AT	*IL6* reverse
TGA TGG CCT TCG ATT CTG GA	*IP10* forward
AGT GGC ATT CAA GGA GTA CC	*IP10* reverse
CAG CCA TGG GCT GGG AC	*ISG15* forward
GCC GAT CTT CTG GGT GAT CT	*ISG15* reverse
AAC AGC GAC TGC ACG TTG AAG G	*ADAM17* forward
CTG TGC AGT AGG ACA CGC CTT T	*ADAM17* reverse
GAC TGT GCA CTT GCT GGT GGA T	*IL6R* forward
ACT TCC TCA CCA AGA GCA CAG C	*IL6R* reverse

CAG AGT TCA CAC CTT ACC TGG AG	*F3* forward
GTT GTT CCT TCT GAC TAA AGT CCG	*F3* reverse
CAG CTC AAT GCT GTG AAT AAC TCC	*TFPI* forward
TCT GCT GGA GTG AGA CAC CAT G	*TFPI* reverse
AAC GAC CTC TGC GAG CAC TTC T	*THBD* forward
CCA GTA TGC AGT CAT CCA CGT C	*THBD* reverse
CTC ATC AGC CAC TGG AAA GGC A	*SERPINE1* forward
GAC TCG TGA AGT CAG CCT GAA AC	*SERPINE1* reverse
CCT TGA ATC CCA GTG ACC CTG A	*VWF* forward
GGT TCC GAG ATG TCC TCC ACA T	*VWF* reverse
AAG TGG AGT CCA GCC GCA TAT C	*CD31* forward
ATG GAG CAG GAC AGG TTC AGT C	*CD31* reverse
GAA GCC TCT GAT TGG CAC AGT G	*CDH5* forward
TTT TGT GAC TCG GAA GAA CTG GC	*CDH5* reverse
ATC GCT GCT GAG TGA ACC ACA G	*CD146* forward
CTA CTC TCT GCC TCA CAG GTC A	*CD146* reverse
GTC CAG AAT CTC GGA AAA GTG CC	*TJP1* forward
CTT TCA GCG CAC CAT ACC AAC C	*TJP1* reverse
AGC GGC TGT ACT GCA AAA ACG G	*FGF2* forward
CCT TTG ATA GAC ACA ACT CCT CTC	*FGF2* reverse
TTG CCT TGC TGC TCT ACC TCC A	*VEGFA* forward
GAT GGC AGT AGC TGC GCT GAT A	*VEGFA* reverse
GGA ACC TCA CTA TCC GCA GAG T	*VEGFR2* forward
CCA AGT TCG TCT TTT CCT GGG C	*VEGFR2* reverse
CAA TGC TGC AAT CGT GCT AC	*SARS-CoV-2 N* forward
GTT GCG ACT ACG TGA TGA GG	*SARS-CoV-2 N* reverse
TCG TTT CGG AAG AGA CAG GT	*SARS-CoV-2 E* forward
GCG CAG TAA GGA TGG CTA GT	*SARS-CoV-2 E* reverse

Appendix Table S2. Commercially available primary antibodies used in this study.

Antibody	Supplier	Catalogue Number	Staining Concentration
anti-mouse proSPC (Rabbit polyclonal)	Abcam	Cat#: ab40879	IF (1:100)
anti- human Podoplanin / gp36 (Mouse monoclonal [18H5]	Abcam	Cat#: ab10288;	IF (1:100)
anti-human von Willebrand Factor conjugated to Alexa 647 (Rabbit monoclonal [EPSISR15])	Abcam	Cat#: ab195029	IF (1:100)
anti-human ZO-1 (Rabbit polyclonal)	Abcam	Cat#: ab216880	IF (1:100)
anti-human CD 31 (Mouse monoclonal [P2B1])	Abcam	Cat#: ab24590	IF (1:100)
anti-human CD 5 (Mouse monoclonal [MEM-28])	Abcam	Cat#: ab8216	IF (1:100)
anti-SARS-COV-2 Spike protein (Mouse monoclonal [1A9])	Genetex	Cat#: GTX632604	IF (1:750)
anti-SARS-COV-2 Nucleocapsid protein (Mouse monoclonal ([6H3])	Genetex	Cat#: GTX632269	IF (1:750)